DOI 10.1007/s10511-016-9427-8
Astrophysics, Vol. 59, No. 2, June, 2016

SINGULAR-SPECTRUM ANALYSIS AND WAVELET ANALYSIS OF THE VARIABILITY OF THE EXTRAGALACTIC RADIO SOURCES 3C 120 AND CTA 102

G. I. Donskikh,[1] M. I. Ryabov,[2] A. L. Sukharev,[2] and M. Aller[3]

This is a study of the variability of the fluxes of radio emission from the quasar CTA 102 and the radio galaxy 3C 120 based on data from the University of Michigan Radio Astronomy Observatory (UMRAO, Ann Arbor). The data were obtained at three frequencies (14.5, 8, and 4.8 GHz) with the 26-m radio telescope. Two mutually complementary methods were used for the analysis: wavelet analysis and singular spectrum analysis. Wavelet analysis is based on the Fourier transform, while singular-spectrum analysis does not use an analyzing function. Long-duration components of the variability in the range of ~4-11 years were found for 3C 120 and ~1.5-3 years, for CTA 102. The short-duration components of the variability are characterized by periods of ~0.7-3.4 years for 3C 120 and ~0.5-0.8 years for CTA 102. These data were also compared with VLBI charts from the MOJAVE archive for studying the evolution of the components in the jets of the quasars studied here.

Keywords: *quasar: radio emission variability: 3C 120, CTA 102*

1. Introduction

The data studied in this paper were obtained during monitoring of extragalactic radio sources at the 26-m radio telescope of the University of Michigan. This monitoring is unique for the duration and continuity of the observations. Observations of the source 3C 120 were made at frequencies of 14.5 (1974-2010), 8 (1966-2010), and 4.8

(1) Department of Astronomy, I. I. Mechnikov Odessa National University, Odessa, Ukraine; e-mail: donskikh.ann@yandex.ua
(2) Institute of Radio Astronomy, National Academy of Sciences of Ukraine, URAN-4 Observatory, Odessa
(3) Department of Astronomy, University of Michigan, Ann Arbor, Michigan, USA

Original article submitted October 12, 2015; accepted for publication March 23, 2016. Translated from Astrofizika, Vol. 59, No. 2, pp. 231-244 (May 2016).

GHz (1980-2009). Observations of CTA 102 were made at all three frequencies from 1999 through 2011. The calibration and data analysis techniques are described elsewhere [1,2].

The radio galaxy 3C 120 (0430+052) is at a distance of 143 Mpc and is of Seyfert 1 type with a red shift z ~ 0.033 [3]. It has a jet that is detectable at optical, radio, and x-ray wavelengths. According to VLBI observations, the visible maximum velocity of the components in the jet is 6.44 c [4]. Precession of the jet in 3C 120 with a period of 12.3 years has been reported [5]. It has been proposed that there are two black holes at the center of the system (the upper bound for the mass of the primary black hole is $3.0 \cdot 10^7 M_{\odot}$ and the lower bound for the mass of the secondary is $4.0 \cdot 10^6 M_{\odot}$). This source has been monitored for many years at the Metsähovi Observatory. Temporal periodicities of 4.3 and 1.4 years at frequencies of 22 and 37 GHz have been discovered [6]. Periods of 0.5 year at 22 GHz and 0.3 year at 37 GHz have also been found. A period of 2.7 years has been detected at 90 GHz.

The quasar CTA 102 (2230+114) is at a distance of 6943 Mpc. It has a red shift of z ~ 1.037 [7]. The visible maximum velocity of the components in the jet is 8.62 c [4]. In 2006 a powerful burst of activity was observed in this source. A shock-in-jet model was proposed to explain this activity [8]. The mass of the central black hole has been estimated to be $5.5 \cdot 10^9 M_{\odot}$ [9]. This source has been observed at the Metsähovi Observatory since 1986. Variability periods of 5.2 and 9.7 years have been found for the flux at 37 GHz; 4.9 and 8.4 years at 22 GHz; 9.2, 8.3 and 4.3 years at 14.5 GHz; and 3.8, 8.5 and 9.8 years at 4.8 GHz [10]. Various approaches are used to study the variability of the fluxes from extragalactic radio sources. The general properties of a large number of radio sources have been studied at 6 frequencies with the RATAN-600 radio telescope [11]. Variabilities on time scales ranging from a few days to several years have been studied. It was indicated [11] that in most of the observed sources the variability is produced by the propagation of a shock wave in a jet.

In order to obtain a detailed picture of the variability of each radio source individually, it is necessary to use data analysis techniques that are capable of solving this problem. These methods include wavelet analysis and singular-spectrum analysis.

2. Initial data and preliminary analysis

In this paper we use data on the fluxes averaged over 7 days. The data were smoothed with a polynomial (second degree) sliding average and trend subtraction to reveal short-period components. Trigonometric interpolation was used to obtain initial data with uniform sampling in time (0.02 year) [12].

A preliminary analysis of the data reveals the existence of trend components in the flux changes and short-duration variations against this background. The subsequent wavelet analysis calculations were done separately for these two components. Initial smoothing of the data from sources 3C 120 and CTA 102 for three frequencies are shown in Figs. 1 and 2.

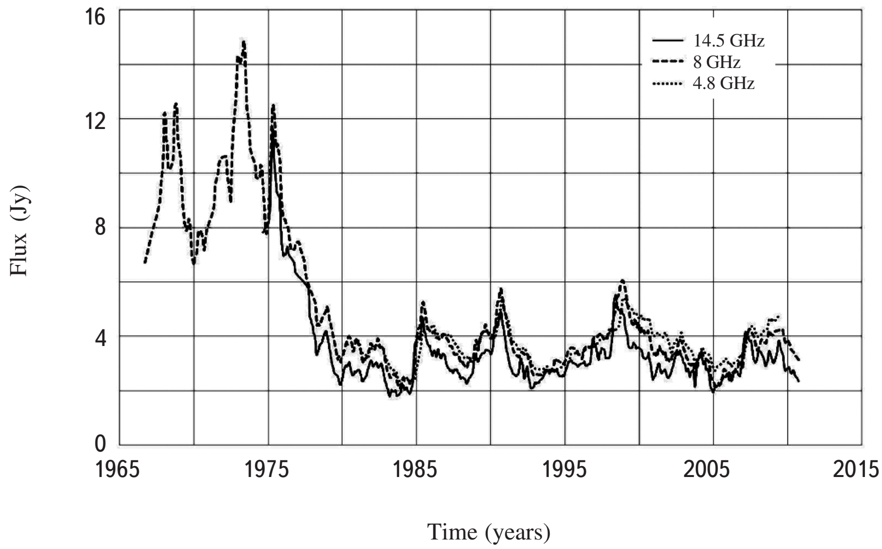

Fig. 1. Flux of the source 3C 120 at frequencies of 14.5 and 4.8 GHz.

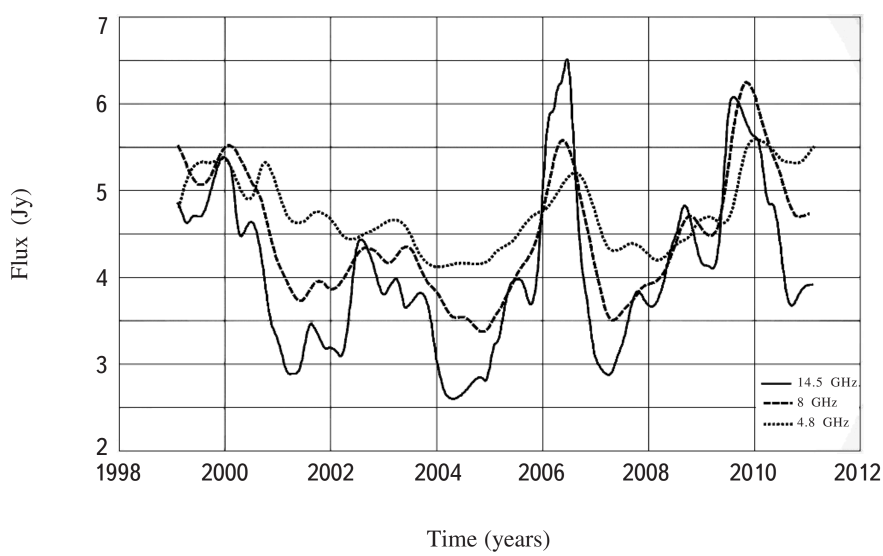

Fig. 2. Flux of the source CTA 102 at frequencies of 14.5, 8, and 4.8 GHz.

3. Wavelet analysis

FFT filtering was applied to the data before wavelet analysis in order to reveal the short-period components.

Wavelet transformation provides a frequency-time representation of the signals. The continuous wavelet transformation is defined by the following equation:

$$W(a,b)=\frac{1}{\sqrt{a}}\int_{-\infty}^{\infty}x(t)\psi^*\left(\frac{t-b}{a}\right)dt\,,$$

where *a* is the scale parameter and *b* is the shift parameter ($a,\ b\in R$, $a\neq 0$). The function $\psi(t)$ is the parent wavelet [13]. The initial function can be recovered using the inverse wavelet transformation:

$$x(t)=C_\psi^{-1}\int_{-\infty}^{\infty}\int_{-\infty}^{\infty}W(a,b)\psi\left(\frac{t-b}{a}\right)\frac{1}{\sqrt{a}}\frac{dadb}{a^2},\quad C_\psi=\int_{-\infty}^{\infty}|\hat{\psi}|^2|\omega|^{-1}\,d\,\omega\,,$$

where C_ψ is an tolerance parameter which must correspond to the tolerance criterion $C_\psi<\infty$.

In this paper we use the Morlet wavelet, which is well localized in terms of time and frequency. The method is described in detail in Refs. 14 and 15. Examples of the application of wavelet analysis for analyzing data from extragalactic sources are described in Ref. 16.

4. Results of using the wavelet method

Examples of frequency-time wavelet spectra on a logarithmic scale for the short-period and trend components are shown in Figs. 3 and 4. Here the harmonic components of the signal can be seen as bright spots along the time axis. Wavelet spectra were used to detect short- and long-time components, as well as their times of appearance and

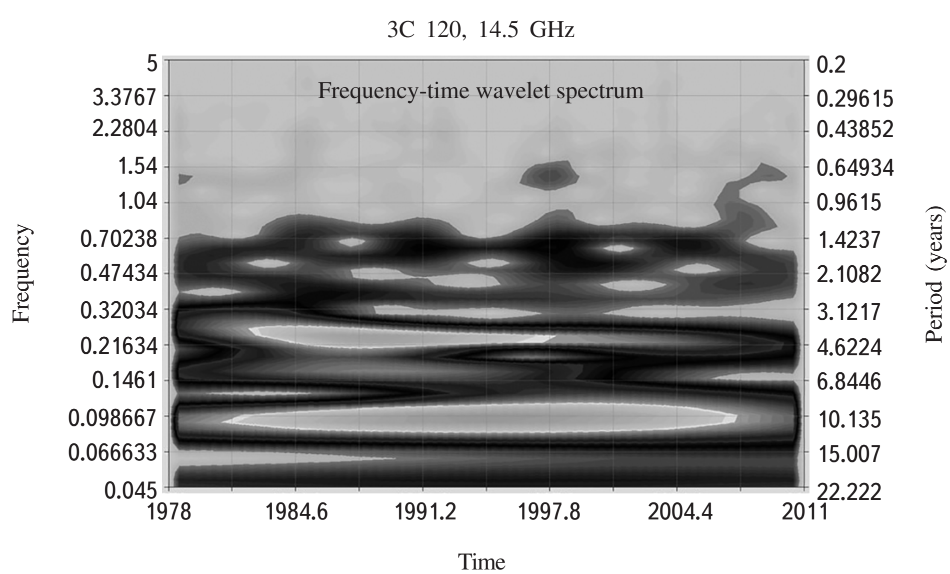

Fig. 3. An example of a wavelet spectrum for the long-time component of the source 3C 120 at 14.5 GHz. Periods of duration ~11 and 4.4 years can be seen in the spectrum.

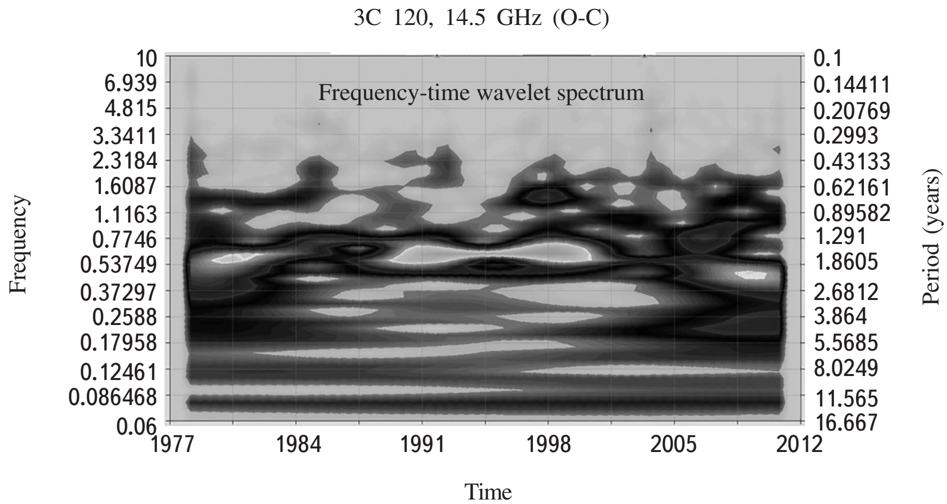

Fig. 4. An example of a wavelet spectrum for the short-time component of the source 3C 120 at 14.5 GHz. Periods of duration ~0.7 and 1.6 years are evident.

durations. The error in determining the periods is ~0.07-0.30 year.

The results of the wavelet analysis for the source 3C 120 are shown in Table 1.

The results of the wavelet analysis calculations for the source CTA 102 are shown in Table 2.

The periods of ~0.7-3.4 years for 3C 120 and ~0.5-0.8 year for CTA 102 are associated with rapid changes in the jet structure. They show up as new components or as motions of existing bright nodes along the jet. Longer lasting periods of 4 to 11 years for 3C 120 and of 1.5 to 3 years for CTA 102 are indicative of activity in the nucleus.

TABLE 1. Results of Wavelet Analysis for the Source 3C 120

Long-time component					
Frequency (GHz)	Period (years)	Start of period	End of period	Maximum spectral power	Dates of maximum spectral power
1	2	3	4	5	6
14.5	10.89	1977	2010	156.4	1992.96
	4.44	1982	2010	149.7	1989.92
8	7.98	1975	2009	480.99	1975.09
	4.44	1967	2009	623.26	1970.93
	2.25	1968	1976	277.69	1973.87
	1.30	1970	1975	110.7	1973.87
4.8	10.90	1980	2009	258.8	1996.84
	4.44	1980	2009	134.42	1987.96

TABLE 1. (Conclusion)

1	2	3	4	5	6
Short-time component					
14.5	1.64	1980 1990	1983 2000	3.79	1997.89
	0.74	1978 1996 2007	1984 2000 2009	2.12	1997.89
8	3.40 3.06	2000 1976	2009 1978	4.54 3.04	2006.97 1977.92
	1.69	1976 1988 1995 2007	1982 1993 1999 2009	3.96	1980.01
4.8	3.40 3.03	1987 1980	2009 1985	1.82 2.28	1987.03 1982.93
	2.69	1986 1992	1989 1994	1.98	1986.09
	1.88	1999	2002	1.53	2000.71
	1.50	1990 2003	1994 2006	2.35	1991.35

The maximum activity for these sources was observed when the appearance times for the activity of the long- and short-time components coincided. The magnitude of the spectral power is greater for the long-time components and corresponds to activity in the "nucleus-accretion disk" system.

An anomalously high activity at 8 GHz was observed for the source 3C 120 during 1966-1975 (this did not happen at the other two observation frequencies during this time), so that the spectral power is highest here.

5. "Period spectra" and comparison with the MOJAVE VLBI charts

Period spectra" were constructed from the wavelet analysis data as period-spectral power plots for each observation year. They can be used to determine the periods that make the largest contribution to the formation of the activity phases of a given source, as well as the time and duration of these phases. These types of data are plotted here on the basis of wavelet analysis for the first time. The period spectra can be used to observe the development

TABLE 2. Results of Wavelet Analysis Calculations for the Source CTA 102

Long-time component					
Frequency (GHz)	Period (years)	Start of period	End of period	Maximum spectral power	Dates of maximum spectral power
14.5	3.1	1999	2011	12.62	2005.97
	1.7	2007	2011	6.99	2007.97
8	3.0	1999	2009	6.5	2005.93
	1.8	2003	2011	3.63	2008.91
4.8	3.5	2004	2011	2.48	2006.95
	1.7	1999	2011	1.13	2007.98
Short-time component					
14.5	0.8	1999	2000	1.92	2005.97
	0.4	2004 2005 2010	2010 2008 -	1.42	2006.32
8	0.9	2000 2007	2003 2008	0.86	2008.97
	0.5	2000 2005	2001	0.47	2005.03
4.8	0.9	2002 2005 2010	2006	0.66	2002.02
	0.7	1999 2008	2000 2009	1.26	2000.49

of the variability dynamics on different time scales.

In order to study the structure of the radio sources during their periods of maximum activity, we have studied VLBI charts for 15.4 GHz from the MOJAVE (Monitoring of Jets in Active Galactic Nuclei with VLBI experiments) archive (for more detail on the MOJAVE project see Ref. 17). The VLBI observations have the disadvantage of being episodic. At the same time, continuous data on the period spectra need spatial identification. The correspondences of the spatial and temporal structure were determined for VLBI data on the same date. As an example, Fig. 5 shows the period spectra of the long- and short-time components for 3C 120 during one of its enhanced activity phases in 1998. An increase in the radio brightness of the VLBI core and a new component in the jet can be seen in the

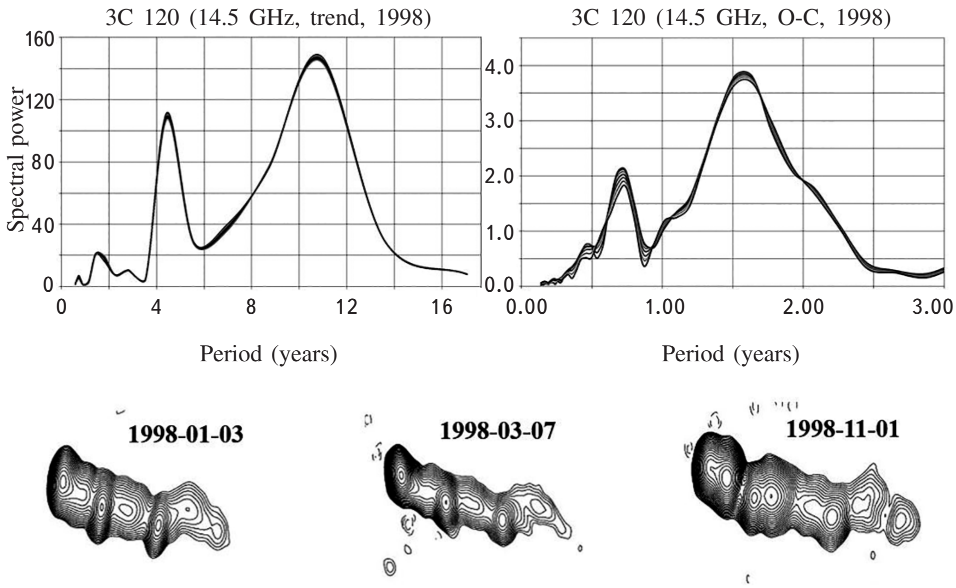

Fig. 5. Comparison of period-spectral density plots at 14.5 GHz with MOJAVE VLBI charts (15.4 GHz) for 3C 120.

MOJAVE VLBI charts. The period-spectral density curves show that periods of ~0.7 and 1.5 years (short-time) and ~4.4 and 11 years (long-time) appeared during this time.

Period spectra and VLBI charts for an activity phase of CTA 102 during 2006 are shown in Fig. 6. The curves

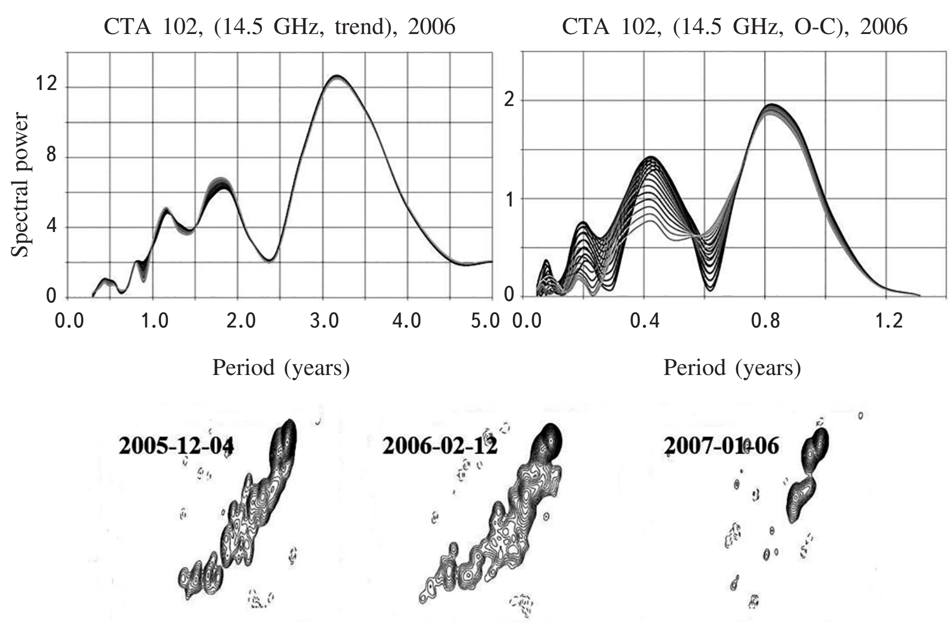

Fig. 6. Comparison of period-spectral density plots at 14.5 GHz with MOJAVE VLBI charts (15.4 GHz) for CTA 102.

show that the major contribution to this activity is from short periods of duration ~0.4 and 0.8 years and from longer periods of ~1.7 and 3.1 years.

A study of the MOJAVE VLBI charts for the jets in these objects revealed a moving component (bright node) and components which are stationary relative to the nucleus for a certain time. In the latter case, as previously proposed [18-20], standing shock waves may be the explanation.

6. Singular spectrum analysis

The data were also analyzed using singular spectrum analysis. This method is based on transforming a one-dimensional time series into a multidimensional series, after which the method of principal components is applied. A singular spectrum analysis decomposes the initial signal into a set of narrowband filters which include trends and periodic components, and noise from the signal. The principal components of the initial matrix can be studied and ordered in terms of their increasing contribution to the original series.

Singular spectrum analysis involves expanding and recovering the initial data series.

6.1. Expansion. The expansion stage includes imbedding and a singular expansion.

Imbedding transforms the initial time series into a sequence of multidimensional vectors. The window length L is an integer $1 < L < N$. Imbedding forms $K = N - L + 1$ imbedding vectors $X_i = \left(f_i, ..., f_{i+L-2}\right)^T$, with $1 \le i \le K$ that have dimensionality L. The trajectory matrix of the series F,

$$X = \left[X_1; ...; X_K\right] \tag{1}$$

consists of the imbedding vectors as columns [21].

Singular expansion. A singular expansion of the trajectory matrix of the series is constructed in this step. Let $S = XX^T$ with $\lambda_1, ..., \lambda_L$ as the eigenvalues of the matrix S, ($\lambda_1 \ge ... \ge \lambda_L \ge 0$) and U_1, … , U_L be an orthonormal system of eigenvectors of the matrix S corresponding to the eigenvalues.

Let $d = \max\{i : \lambda_i > 0\}$; if $V_i = X^T U_i \big/ \sqrt{\lambda_i}$, with $i = 1$, …, d, then the singular expansion of the matrix S will be

$$X = X_1 + ... + X_d , \tag{2}$$

where $X_i = \sqrt{\lambda_i}\, U_i V_i^T$. The set ($\sqrt{\lambda_i}$, U_i, V_i) is the i-th eigen-triplet of the singular expansion (2).

6.2. Recovery. The recovery procedure includes grouping and diagonal averaging. *Grouping.* The additive components of the series are separated by grouping. Based on the singular expansion state (2), grouping divides the set of indices $\{1, \ldots, d\}$ into m nonintersecting subsets $I_1, \ldots, I_m$.

Let $I = \{i_1, \ldots, i_p\}$. Then the resulting matrix X_I is defined as $X_I = X_{i_1} + \ldots + X_{i_p}$. The expansion (2) can be written in the grouped form

$$X = X_{I_1} + \ldots + X_{I_m} . \qquad (3)$$

The procedure for choosing the sets $I_1, \ldots, I_m$ is grouping of the eigen-triplets.

Diagonal averaging. In this stage, each matrix of the grouped expansion (2) is converted into a new series of length N.

On applying diagonal averaging to the matrixes X_{I_k}, we obtain the series $\tilde{F}^{(k)} = \left(\tilde{f}_0^{(k)}, \ldots, \tilde{f}_0^{(k)}, \ldots, \tilde{f}_{N-1}^{(k)}\right)$. The initial series $(f_0, \ldots, f_{N-1})$ is expanded in the form

$$f_n = \sum_{k=1}^{m} \tilde{f}_n^{(k)} . \qquad (4)$$

Singular spectrum analysis is described in greater detail in Ref. 21.

The periodic components of the series being studied form a pair of neighboring components. Some examples of the principal components obtained by singular spectrum analysis of the source CTA 102 at 8 GHz are shown below (Figs. 7 and 8).

The distinctive feature of singular spectrum analysis is that its calculations do not use an analyzing function, so these calculations make it possible to isolate the different components of the series with great accuracy. In order to get an idea of the time evolution of the spectral power of the test signal, a windowed Fourier transform or short-period Fourier transform [13] was applied to the narrow-band components calculated by singular spectrum analysis.

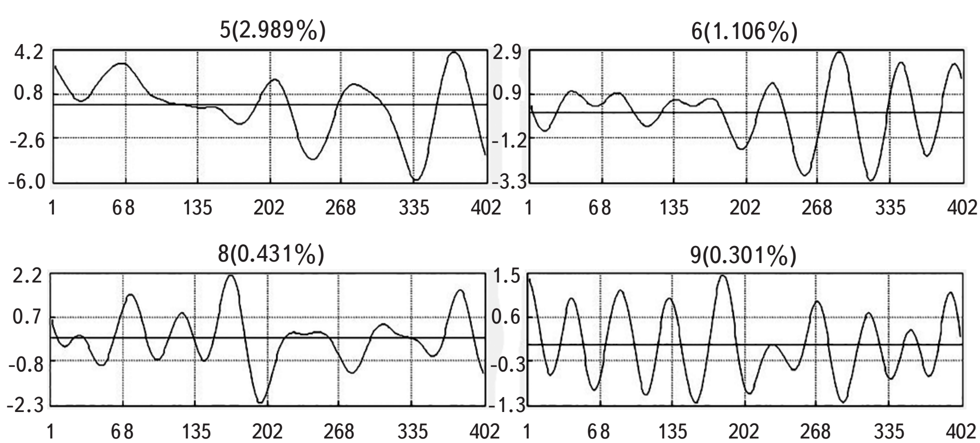

Fig. 7. Principal components of the singular expansion of the trajectory matrix of the series (one-dimensional diagrams) for CTA 102 at 8 GHz.

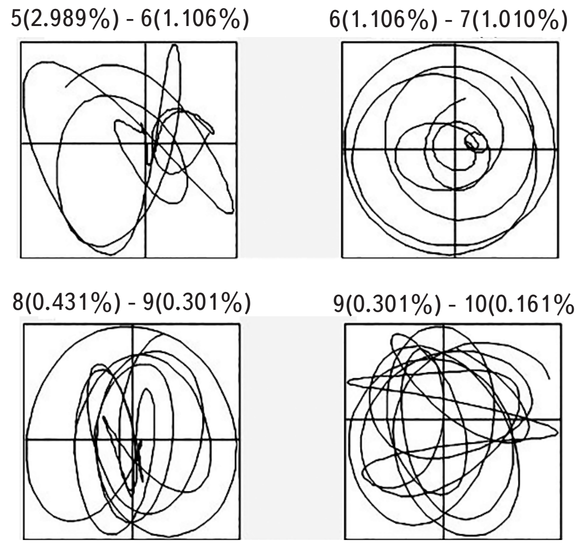

Fig. 8. Principal components (two-dimensional diagrams) for CTA 102 at 8 GHz.

When the windowed Fourier transform is used, the signal is divided into segments (“windows”), within each of which it is assumed to be stationary. A window function with a width equal to the width of the window is added to the signal. The windowed Fourier transform (WFT) is the Fourier transform of the signal multiplied by the window function. The WFT can be written as

$$F(t,\omega)=\int_{-\infty}^{\infty} f(\tau)W(\tau-t)e^{-i\omega\tau}d\tau,$$

where $W(\tau-t)$ is a window function.

By calculating the short-time Fourier transform for each component obtained during the singular spectrum analysis, it is possible to obtain the spectral power of this component over time.

The results of singular spectrum analysis for the sources studied here are listed in Table 3.

In Table 3 the dates of maximum activity are underlined and these coincide for several periods. The amplitude peaks of the radio flux at different frequencies are the result of time coincidence of the different periodic components.

7. Conclusions

Singular spectrum analysis and wavelet analysis can be used to obtain a detailed picture of the development of the variability in the fluxes of extragalactic radio sources. As a whole, most studies of the variability of the radio fluxes from extragalactic radio sources have identified the major periods over the entire time interval. In this paper,

TABLE 3. Results of Singular Spectrum Analysis for 3C 120 and CTA 102

Frequency (GHz)	3C 120		CTA 102	
	Period (years)	Date of max. activity	Period (years)	Date of max. activity
14.5	8.0	1975.2, 1990.9, 2007.9	2.7	2004.7, 2007.5
	4-4.8	1990.9, 1992.5, 1996.8, 2003.7, 2007.8	2.0	2005.7, 2006, 2007.1, 2008.7, 2010.5
	6.0	1975.9, 2008.9	1.3	2006, 2008.7, 2009
	2.7	1977.7, 1979, 1991, 1995.6, 2005.7, 2008.1	1.1-1.2	2002, 2003.9, 2005, 2006.6, 2007.7, 2008.5, 2009, 2010.5
	1.6	1975.3, 1992.2	1.0	2005.9, 2006.9, 2008.7, 2009.5
			0.8	2003.2, 2005.9, 2006, 2010.5
8	7.4	1971.1, 1973, 1991	4.0	2010.5
	5.9	1995.6, 1999.2, 2008	2.7	2001.9, 2005.9
	4.2	1971.1, 1972.9, 1973, 1991, 1999.9, 2000.5	2.0	2009.5
			1.6	2002.4, 2008.7
	3.3	1972.9, 1999.4	1.15	2001.9, 2007.1, 2008.5, 2009.6, 2010.5
	1.97	1973, 1990.3, 1991, 1999.7		
	1.74	1973, 1999.9	0.6-0.9	2001.9, 2003.1, 2007.1, 2008.4
4.8	9.7	1988.1	3.5	2002.7
	6.5	1984.8, 2000.7, 2004.1	2.3	2005.9
	4.85	2000	1.4	2003.9
	3.2	2000.3	1.0	2003.9, 2004.1, 2008, 2009.7
	2.8	1984.8, 1990.9, 1999.9, 2000.7, 2005.2	0.5-0.7	2003.5, 2004.1, 2005.2, 2010.1
	1.9	2000.3		
	1.4	2000, 2001.9, 2005.7		

we have studied the major periods and the times at which they appear. The appearance of the activity presents a rather complicated picture that reflects the variety of processes involved. These data can provide a complete picture of the variability on different time scales, so in the future it will be possible to create a physical model of the variability in agreement with the observational data.

Comparisons with data from episodic VLBI observations make it possible to relate these processes to changes in the spatial and angular structure of a radio source. We have discovered long-time components of the variability in ranges of ~4-11 (3C 120) and ~1.5-3 years (CTA 102) associated with activity of the nucleus in these extragalactic sources. For the short-time variable component associated with activity of a jet, the typical periods are ~0.7-3.4 (3C 120) and ~0.5-0.8 years (CTA 102). Singular spectrum analysis calculations of the periodicity of the fluxes of the extragalactic sources have been compared with the results of wavelet analysis. The results of the two different methods for analyzing the time series were in good agreement. For long data series, the computational time for the wavelet method is considerably shorter than for singular spectrum analysis. Singular spectrum analysis provides a more precise determination of the periods of the variability than wavelet analysis. The data have been compared with VLBI charts from the MOJAVE project in order to study the variation in the structure of the jets and to relate these changes to the appearance of certain periods. The complicated pattern of the variability in the fluxes from these sources is the basis for "nucleus-accretion disk-jet" models of active galactic nuclei and for representing the dynamics of their development.

REFERENCES

1. M. F. Aller, H. D. Aller, and P. A. Hughes, Bull. American Astron. Soc. **33**, 1516 (2001).
2. P. A. Hughes, H. D. Aller, and M. F. Aller, Astrophys. J. **396**, Part 1, 469 (1992).
3. A. Michel and J. Huchra, Publ. Astron. Soc. Pacif. **100**, 1423 (1988).
4. M. L. Lister, M. F. Aller, H. D. Aller, et al., Astron. J. **146**, 22 (2013).
5. A. Caproni and Z. Abraham, Mon. Not. Roy. Astron. Soc. **349**, 1218 (2004).
6. T. Hovatta, H. J. Lehto, and M. Tornikoski, Astron. Astrophys. **488**, 897 (2008).
7. R. Falomo, R. Scarpa, and M. Bersanelli, Astrophys. J. Suppl. Ser. **93**, 125 (1994).
8. C. M. Fromm, M. Perucho, E. Ros, et al., Astron. Astrophys. **531**, 14 (2011).
9. S. Zhang, W. Collmar, V. Schoenfelder, et al., http://arXiv:astro-ph/0107173 (2001).
10. N. A. Kudryavtseva and T. B. Pyatunina, A Search for Periodicity in the Light Curves of Selected Blazars, http://arXiv:astro-ph/0511707v1 24 Nov (2005).
11. A. G. Gorshkov, V. K. Konnikova, and M. G. Mingaliev, Astron. zh. **89**, 388 (2012).
12. A. L. Sukharev and M. F. Aller, Odessa Astron. Publ. **27**, 78 (2014).
13. R. Polika, Introduction to the Wavelet Transformation, translated by V. G. Grinbuhin, AVTEKS (2013), 59 pp.
14. I. Dobesi, Ten Lectures on Wavelets [translated from English], NITs "Regulyarnaya i khaoticheskaya dinamika," Izhevsk (2001), 464 pp.
15. V. V. Vityazev, Wavelet Analysis of Time Series: A Textbook, Izd-vo S.-Peterb. un-ta., St. Petersburg (2001), 58 pp.
16. A. L. Sukharev and M. F. Aller, Odessa Astron. Publ. **26**, 256 (2013).
17. M. L. Lister, et al., Astron. J. **138**, 1874 (2009).

18. S. Jorstad, A. P. Marscher, J. R. Mattox, et al., Astrophys. J. Suppl. Ser. **134**, 181 (2001).
19. S. Britzen, R. C. Vermeulen, R. M. Campbell, et al., Astron. Astrophys. **484**, 119 (2008).
20. A. Alberdi, J. L. Gómez, J. M. Marcaide, A. P. Marscher, and M. A. Pérez-Torres, Astron. Astrophys. **361**, 529 (2000).
21. N. E. Golyandina, The "Caterpillar"-SSA Method: Time Series Analysis (a Textbook), Izd. S.-Peterb. un-ta., St. Petersburg (2004), 74 pp.